A Comparative Study Between Proton and Neutron Induced SEUs in SRAMs

Thomas Granlund and Nils Olsson

***Abstract*—We report on irradiation induced SEU by high-energy protons and neutrons. The experiments were performed at The (odor) Svedberg Laboratory in Uppsala, Sweden, and at the Weapons Neutron Research (WNR) facility, Los Alamos, USA. A wide range of SRAMs were used to study the differences between proton and neutron induced SEUs at different energies.**

***Index Terms*—Neutron, proton, SEU, SRAM, WNR.**

I. Introduction

THE neutron is a prevailing particle in our atmosphere at passenger aircraft cruising altitudes. It is also the dominating source of Single-Event Effects at these altitudes [1]. Neutrons originate from spallation reactions, initiated when galactic cosmic rays and solar particles collide with nuclei of oxygen and nitrogen in the atmosphere. The outcome is a cocktail of particles including pions, muons, electrons, gamma rays, protons, and neutrons [2].

The galactic cosmic radiation, submerging the earth, consists of about 88% protons, 9% helium ions, 1% heavier particles, and 2% electrons [3]. Both protons, helium ions and heavier elements are notoriously known for their harsh impact on semiconductor electronics in space [4]. Not only do protons exist in this continuous flow, but they are numerous also in the radiation belts [5] around the Earth and during outbursts from the Sun in so-called solar events [6]. Thus, protons are of great concern in space, regarding SEUs.

There exist only a few neutron acceleration test facilities for device testing compared to the number of proton acceleration test facilities. This makes it inconvenient and hard for potential customers, e.g., the avionic and semiconductor industry, to perform their device testing with little notice.

In this work we therefore investigate the differences between proton and neutron acceleration testing on SRAM devices. A most suitable facility for this purpose is The(odor) Svedberg Laboratory (TSL), that delivers both mono-energetic protons and quasi-mono-energetic neutrons at high fluxes for a wide energy range [7]. The Los Alamos neutron facility, the Weapons Neutron Research (WNR) facility [8], was used as a reference source to compare with the results gained at TSL.

- All samples are of industrial standard.

Manuscript received September 16, 2005. This work was supported in part by the Swedish Defence Materiel Administration (Acknowledgment to Gunnar Ericson).

T. Granlund was with the Electromagnetic Technology Division at Saab Avionics AB, Linköping, Sweden, which is now reorganized within the Communication Division at AerotechTelub AB, Linköping, Sweden. (e-mail: thomas.granlund@aerotechtelub.se).

N. Olsson is with the Systems Technology Division, Swedish Defence Research Agency, Stockholm, Sweden (e-mail: nils.olsson@foi.se).

Digital Object Identifier 10.1109/TNS.2006.880931

TABLE I
TESTED SRAM'S

Sample	Date Code	Speed (ns)	Size (bit)	Voltage (V)	PT (μm)	Comments*
A1	0223	70	1M	3.3	0.25	Fab4/R52LD-3
A2	0036	85	4M	1.8	0.25	Fab4/R52FD-3
A3	0225	70	4M	3.3	0.16	Fab/R7LD-3R
A4	0223	70	8M	2.5	0.16	Fab/R7LD-3R
A5	0221	70	4M	1.8	0.16	Fab4/R7LD-1.8
A6	0151	70	4M	1.8	0.16	Fab4/R7LD-1.8
A7	0311	70	8M	1.8	0.13	Fab/RAM8NLD-1.8
B8	0251	55	8M	3.0	0.13	
C9	0307	70	4M	5.0	0.13	

II. Experimental

A. Devices Under Test

All samples were commercial low power SRAMs of bulk technology hosted in small ball grid array packages. These SRAMs are presented in Table I together with some important data. The letter in the first column marks the manufacturer, which is A, Cypress, B, Hitachi, and C, Samsung. The largest fraction of samples was from Cypress. The samples are, in consecutive order starting from the top of Table I: CY62127BVLL-70BAI, CY62147V18LL-85BAI, CY62147CV33LL-70BAI, CY62157CV25LL-70BAI, CY62137CV18LL-70BAI, CY62147CV18LL-70BAI, CY62157DV18LL-70BAI, HM62V16512LBPI-5SL, and K6X4016C3F-TB70.

The tested device quantity of each sample was 4 to 8 individual devices.

B. Experiment

The accelerated testing, both with neutrons and protons, was performed at The Svedberg Laboratory in Sweden during spring time of 2004 and 2005. A monitoring computer was connected, via coaxial cables, to the experimental set up, in the so-called "blue hall", where the accelerated testing took place. The experimental test set up hosted up to 4 consecutive boards, each containing 2 devices, resulting in simultaneous testing of 8 devices. The distance between two consecutive boards was 10 cm. When testing with protons only one board at a time was in the beam, in order to have the same particle energy impinging on each and every board.

The device memory area was preloaded with ones and zeros in a checkerboard pattern, and continuously updated during testing. When testing SRAMs the choice of pattern is particular important when studying multiple bit upset, but for single bit upset it is of less importance [9]. The memories were continuously checked and updated during the whole test and the detected errors were safely logged onto the hard disk of the

monitoring computer during the whole radiation test. The data logged were the erroneous word, its address and the time of detection.

The beam diameter measured at the test area was 8 cm and 13 cm for the proton and the neutron beams, respectively.

The irradiation was done normal to the sample surface, i.e., onto the top front surface. All samples were placed well inside the beams.

The neutron testing in 2002 and 2003 [10], [11], using the white beam at the WNR facility in Los Alamos, was performed in the same manner as at TSL. The neutron beam diameter at Los Alamos was approximately 8 cm.

At both test facilities the testing involved uncertainties of both systematic and statistical nature. The systematic errors include uncertainties in the neutron (10%) and proton fluences (15%), and the statistical errors originate from the number of SEUs, which were below 8% for neutrons and below 6% for protons at all energies. The reduction in fluence due to boards up streams has been accounted for, both by monitoring the number of SEUs on each board and by calculations at each neutron energy. The processing of the TSL data adds one more source of error, which is linked to the correction procedure of the neutron SEU cross section. This error has not been included in the calculation, in order not to complicate the proton vs. neutron SEU cross-section comparison.

The total neutron- and proton fluence, for each device, was kept below $5 \cdot 10^{10}$ cm^{-2} at all times.

C. Neutron SEU Cross Section at TSL

The raw neutron SEU cross section (σ_{RAW}), for each neutron peak energy, is simply calculated using the following:

$$\sigma_{\mathrm{RAW}} = \frac{\#\mathrm{SEUs}}{\mathrm{Fluence} \cdot \#\mathrm{bits}}. \tag{1}$$

The neutron fluence used in (1) is the fluence within the quasi-mono-energetic peak of the neutron spectrum, and not the whole spectrum. Thus, this is an upper limit for the neutron cross section. A more correct neutron SEU cross section must take into account the low-energy tail of the quasi-mono-energetic neutron spectra. This procedure has been thoroughly documented elsewhere [10]. In short one uses the following:

$$\#\mathrm{SEU} = \int_0^{E_{\mathrm{Peak}}} f\{\sigma(E_{\mathrm{Peak}})\} \cdot \frac{dN}{dE} \cdot dE \tag{2}$$

where f is a function of the cross section adjusted to fit the number of SEUs actually measured at the energy in question. The last term on the right hand side is the differential neutron fluence spectrum from the actual test run at TSL, see Fig. 1.

The function f may be expanded into to two terms

$$f\{\sigma(E_{\mathrm{Peak}})\} = \sum_i \sigma_{\mathrm{RAW}}(E_{\mathrm{Peak}}(i)) \cdot C_{\mathrm{tail}}(E_{\mathrm{Peak}}(i)) \tag{3}$$

where the constant C_{tail} is chosen so (2) is fulfilled at each tested neutron energy i. Thus, for each and every tested peak neutron energy i a C_{tail} value is given. C_{tail} corrects for the σ_{RAW} non mono-energetic origin. Each experimental cross section point i is connected to the next consecutive cross section point by a straight line. The assumed threshold energy is connected through a straight line to the first cross section point, i.e., the cross section point at the lowest neutron energy ($i = 1$), and after the last cross section point the cross section is assumed to be constant at the same value as the last cross section point.

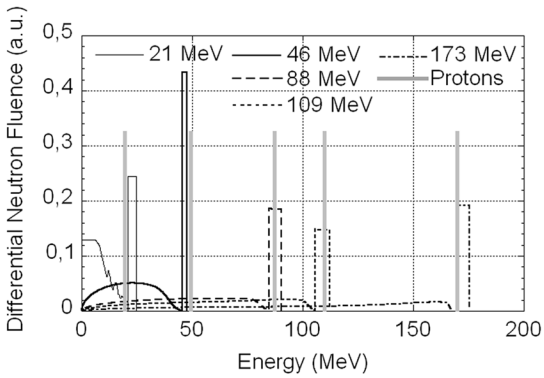

Fig. 1. Differential neutron spectra for all five energies used. The spectra are normalized to unity within the peak. For the proton beam, here schematically sketched, the energies use were: 19, 49, 87, 110, and 170 MeV.

D. Differential Neutron Spectrum at TSL

The neutron spectra from TSL are calculated and not experimentally determined. Experimental data exist in the 20–150 MeV energy region, and they confirm the systematics [12], [13]. However, experimental data at medium energies, i.e., around 173 MeV, do not exist (see [12] and references therein). Two models [12], [13] have been used to calculate the neutron spectra. For the neutron spectrum below 45 MeV, results from Mashnik *et al.* [13], obtained with the GNASH code and included in the LA150 library [14], were used. Using this model above 45 MeV will cause major disagreement with experimental data as shown in paper [12]. Instead, the semi-empirical systematical analysis of all available experimental data, as presented by Prokofiev *et al.* [12] is used for the incident proton energies above 45 MeV (before target). The results are shown in Fig. 1, for all five neutron energies used here.

III. Results and Discussion

A. TSL Results

The SEU cross-section results from TSL are shown in Fig. 2, which includes the raw neutron SEU cross section, by definition the upper limit for the true neutron SEU cross section, the corrected cross section for one of the two chosen thresholds (1 MeV and 5 MeV), and the proton SEU cross section. For lucidity, the energy threshold is included along with the experimental results in Fig. 2. The soft error rate (SER) values may then be calculated directly from Fig. 2. The lowest neutron energy used in the experiment was 21 MeV. Worth noting is that the decrease of the SEU cross section towards zero is assumed here to be linear, but this may not be the case in reality.

The proton SEU cross section typically rises to 46 MeV, then decreases and flattens out at higher energies. The raw and corrected SEU cross section for neutrons rises and flattens

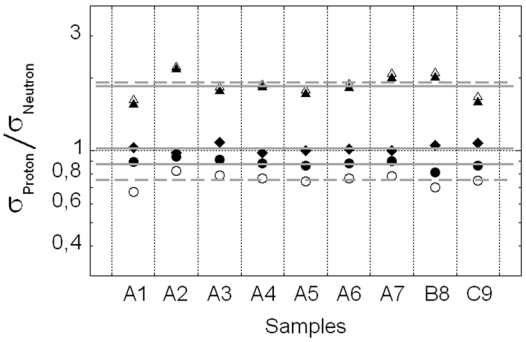

Fig. 2. SEU cross sections, for all samples, displaying the raw neutron SEU cross section (dash-dot-line), the corrected neutron SEU cross section with energy threshold of 1 MeV (solid line) and the proton SEU cross section (dotted line).

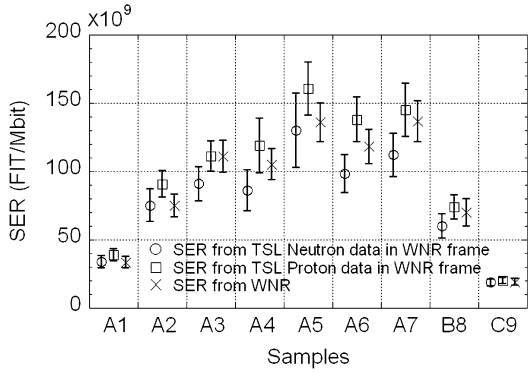

Fig.–3. SEU cross-section ratio between protons and neutrons at 21 MeV with energy threshold of 1 MeV (filled circle) and 5 MeV (empty circle), and 46 MeV with energy threshold of 1 MeV (filled triangle) and 5 MeV (empty triangle), and at 88 MeV with energy threshold of 1 MeV (filled diamonds) and 5 MeV (empty diamonds, not seen due to overlap with 1 MeV filled diamonds). The solid gray lines indicates the average value for thresholds of 1 MeV and dashed gray line the average value for thresholds of 5 MeV for each of the three energies.

out without a sharp, pronounced peak. Moreover, the proton and corrected neutron SEU cross sections coincide at 88 MeV and linger closely together above this energy. This is what is expected at higher energies, where the Coulomb barrier for protons should be of minor importance.

Two SEU energy thresholds were chosen, one high, at 5 MeV, and one low, at 1 MeV, in order to see the impact of two possible thresholds. The correct threshold lay most likely between these values according to simulations. Fig. 3 shows the result of a comparison between the proton SEU cross section and the neutron SEU cross section at 21 MeV (circles), 46 MeV (triangles) and 88 MeV (diamonds). At 88 MeV the average value for the cross-section ratio is very close to one (≈ 1.02). This is not the case at 21 MeV, as expected; due to Coulomb forces, it is less than one. The average value at 21 MeV is smaller for an energy threshold of 5 MeV (≈ 0.75) than for that of 1 MeV (≈ 0.88). Thus, the value for a threshold of 5 MeV may be regarded as a lower limit and that for 1 MeV as an upper limit.

At the energy in between 21 MeV and 88 MeV, i.e., at 46 MeV, the difference between the proton cross section and the neutron cross section is at maximum, which was not expected. The sharp peak observed in the proton SEU cross-section curve at 49 MeV is seen for all samples. A similar behaviour of the proton SEU cross section has also been observed by others [15]. C. Dyers data [15] was collected at another irradiation facility, the Tri-University Meson Facility (TRIUMF) [16], and not at TSL. Moreover, the neutron and proton SEU cross sections at around 46 MeV can in no way coincide, because the proton data at 49 MeV reach the corresponding raw neutron cross-section points, which should be approximately twice the level of the corrected SEU cross section. One possible explanation for this discrepancy might be that neutrons and protons interact with silicon in a slightly different way, creating different sets of secondary ions in the SRAMs. Moreover, the neutron SEU cross section might be slightly underestimated by the correction procedure [10]. However, Fig. 3 indicates that the difference at this energy is around 1.9 times.

B. TSL SER Values in WNR Frame

The SER of all the samples may now be calculated for a given flux and neutron spectrum, after making two assumptions, the first: beyond the last measured point the cross section is constant, and of the same value as the last measured point, and the second assumption: the energy threshold is set to 1 MeV or 5 MeV. For comparison, the "white" neutron beam at WNR has been chosen. The white neutron spectrum was provided by WNR for each and every run we conducted at WNR on all samples presented here. The energy threshold of the WNR spectrum is 1 MeV. The SER is simply calculated by folding the cross sections in Fig. 2 with the WNR neutron beam spectrum at a flux of 1E6 neutrons per cm^2 and second (this is a standard neutron flux at WNR). This is done by the following:

$$\mathrm{SER} = \int_{1\ \mathrm{MeV}}^{800\ \mathrm{MeV}} \sigma_{\mathrm{SEU}} \cdot \left.\frac{dN}{dE}\right|_{\mathrm{WNR}} \cdot dE \qquad (4)$$

where σ_{SEU} is the SEU cross section and the second term in (4) is the WNR neutron flux spectrum.

The results, using proton and neutron cross sections with an energy threshold of 1 MeV, are presented in Fig. 4 together with SER values obtained by irradiation at WNR.

Fig. 4 shows that the proton cross section agrees rather well with the WNR SER for all samples. It might be slightly overestimating the SER, but the error bars for WNR SER and TSL SER, based on the proton SEU cross sections, overlap very well. The SER calculated from the neutron SEU cross—sections, follow the WNR SER nicely, but may, contrary to the SER calculated from the proton data, slightly underestimate the SER. However, once again the error bars do overlap here as well.

IV. Conclusion

Energy dependent SEU cross sections, obtained from a quasi-monoenergetic neutron source, may be replaced by SEU cross section measured with a mono-energetic proton source with little error. This was concluded from comparing SER results from TSL with those from WNR.

In addition to nuclear forces, the proton also interacts via Coulomb forces, while the neutron does not, and this fact seems here to be manifested as a 10 to 25% drop in the proton

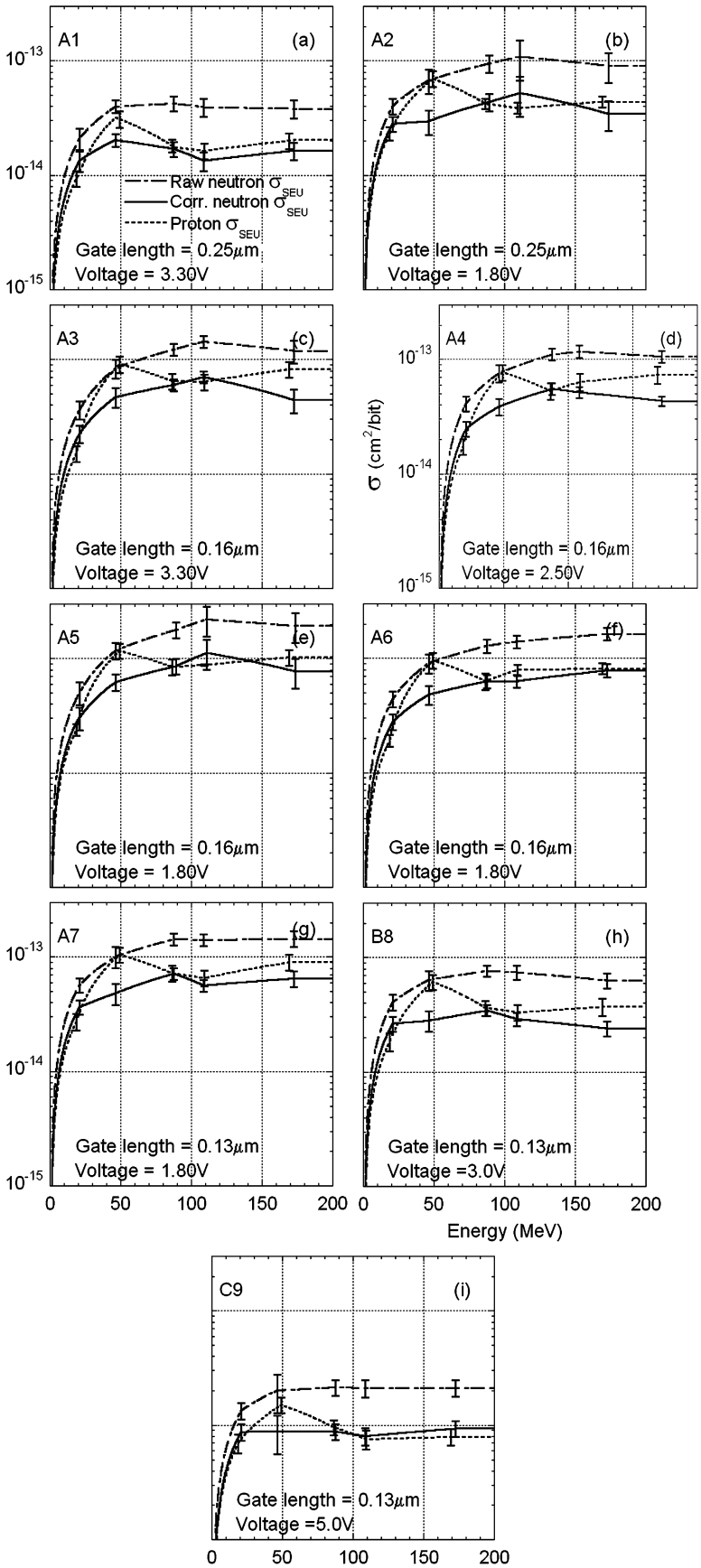

Fig. 4. SER values of each SRAM from WNR testing (cross) and from folding the WNR neutron beam spectrum with both the TSL SEU neutron cross sections (circle) and TSL proton cross section (square). The SER values are per 1 Mbit of memory.

SEU cross section at 21 MeV, compared to the neutron SEU cross—section, after correction for the neutron low-energy tail of the quasi mono-energetic neutron spectrum. At 88 MeV, the SEU cross-section values, induced by protons and neutrons, are very similar. Surprisingly, at energies between 21 and 88 MeV, i.e., here at 46 MeV, the disagreement between proton and neutron SEU cross sections is at maximum. Small differences in the nuclear reactions between silicon and a neutron or a proton may be responsible for this discrepancy, while some part may be attributed to uncertainties in the correction procedure for the cross sections taken with the quasi-mono-energetic neutron source.

ACKNOWLEDGMENT

The authors would like to thank A. Prokofiev for his expertise in both practical theoretical matters, and member of the staff in the control room for their effort to deliver a continuous and steady beam.

REFERENCES

[1] E. Normand and T. J. Baker, "Altitude and latitude variations in avionics SEU and atmospheric neutron flux," *IEEE Trans. Nucl. Sci.*, vol. 40, no. 6, pp. 1484–90, Dec. 1993.

[2] J. F. Ziegler, "The terrestial cosmic ray intensities," *IBM J. Res. Develop.*, vol. 42, no. 1, pp. 117–39, 1998.

[3] T. K. Gaisser, *Cosmic Rays and Particle Physics*. Cambridge, U.K.: Cambridge Univ. Press, 1990.

[4] D. Binder, E. C. Smith, and A. B. Holman, "Satellite anomalies from galactic cosmic rays," *IEEE Trans. Nucl. Sci.*, vol. NS-22, no. 6, pp. 2675–80, Dec. 1975.

[5] M. S. Gussenhoven, E. G. Mullen, and D. H. Brautigam, "Improved understanding of the earth's radiation belts from the CRRES satellite," *IEEE Trans. Nucl. Sci.*, vol. 43, no. 2, pp. 353–68, Apr. 1996.

[6] M. A. Shea and D. F. Smart, "A summary of major solar proton events," *Sol. Phys.*, vol. 127, no. 2, pp. 297–320, 1990.

[7] S. Pomp, A. V. Prokofiev, J. Blomgren, O. Byström, C. Ekström, N. Haag, A. Hildebrand, C. Johansson, O. Jonsson, P. Mermod, L. Nilsson, D. Reistad, N. Olsson, P.-U. Renberg, M. Österlund, U. Tippawan, D. Wessman, and V. Ziemann, "The new uppsala neutron facility," presented at the Int. Conf. Nuclear Data for Science Technology, Santa Fe, NM, Oct. 2004.

[8] P. A. Lisowski, C. D. Bowman, G. J. Russell, and S. A. Wender, "The los alamos national laboratory spallation neutron sources," *Nucl. Sci. Eng.*, vol. 106, pp. 208–18, 1990.

[9] J. F. Ziegler and H. Puchner, *SER-History, Trends and Challenges: A Guide for Designing with Memory ICs*. San Jose, CA: Cypress Corp., 2004.

[10] T. Granlund, B. Granbom, and N. Olsson, "A comparative study between two neutron facilities regarding SEU," *IEEE Trans. Nucl. Sci.*, vol. 51, no. 5, pp. 2922–26, Oct. 2004.

[11] T. Granlund, B. Granbom, and N. Olsson, "Soft error rate increase for new generations of SRAMs," *IEEE Trans. Nucl. Sci.*, vol. 50, no. 6, pp. 2065–8, Dec. 2003.

[12] A. V. Prokofiev, M. B. Chadwick, S. G. Mashnik, N. Olsson, and L. S. Waters, *J. Nucl. Sci. Technol.*, no. Supplement 2, pp. 112–15, 2002.

[13] S. G. Mashnik, M. B. Chadwick, P. G. Young, R. E. MacFarlane, and L. S. Waters, LANL Rep. LA-UR-00-1067, 2000.

[14] M. B. Chadwick, P. G. Young, S. Chiba, S. C. Frankle, G. M. Hale, H. G. Hughes, A. J. Koning, R. C. Little, R. E. MacFarlane, R. E. Prael, and L. S. Waters, "Cross-section evaluations to 150 MeV for accelerator-driven systems and implementation in MCNPX," *Nucl. Sci. Eng.*, vol. 131, pp. 293–328, 1999.

[15] C. S. Dyer, S. N. Clucas, C. Sanderson, A. D. Frydland, and R. T. Green, "An experimental study of single-event effects induced in commercial SRAMs by neutrons and protons from thermal energies to 500 MeV," *IEEE Trans. Nucl. Sci.*, vol. 51, no. 5, pp. 2817–24, Oct. 2004.

[16] E. W. Blackmore, "Operation of the TRIUMF (20–500 MeV) proton irradiation facility," in *Proc. IEEE Radiation Effects Data Workshop Rec.*, 2000, pp. 1–5.